Pergamon International Journal of Machine Tools & Manufacture 38 (1998) 1289–1304

INTERNATIONAL JOURNAL OF MACHINE TOOLS & MANUFACTURE DESIGN, RESEARCH AND APPLICATION

Applied mechanics in grinding—VI. Residual stresses and surface hardening by coupled thermo-plasticity and phase transformation

M. Mahdi, L. Zhang*

Department of Mechanical and Mechatronic Engineering, The University of Sydney, NSW 2006, Australia

Received 12 September 1997

Abstract

The present study aims to investigate the residual stresses and surface hardening in ground components caused by the coupled effect of thermo-plasticity and phase transformation. A feasible numerical method was developed to accommodate appropriately the phase transformation in a workpiece experiencing critical temperature variation during grinding. The change of material properties was modelled as a function of temperature history. It found that if material properties are temperature-independent, the residual stresses in both the grinding direction and that perpendicular to it are tensile. The maximum residual stress in this case does not vary with the further increment of grinding heat. When material properties are temperature-dependent, however, the rise of grinding temperature promotes surface hardening and increases the maximum residual stress. The study showed that the volume growth associated with phase change plays an important role in the formation and nature transition of residual stresses. Nevertheless, residual stresses in the no-martensite zone is nearly unaffected by surface hardening and volume change. This paper offers insight into the understanding of surface hardening mechanism introduced by grinding.

Keywords: Residual stresses; Grinding thermo-plasticity; Phase transformation; Coupling

Notation

B	strain displacement matrix
Cr_{700}	cooling rate at 700°C

* Corresponding author.

0890-6955/98/$19.00
PII: S0890-6955(97)00134-X

$\mathbf{D}$	constitutive matrix, defined by Eq. (4)
D	non-dimensional martensite depth, $2\,d/L_c$
d	martensite depth
H	non-dimensional heat transfer coefficient, $2\alpha h/\kappa v$
h	convection heat transfer coefficient of coolant
H_v	Vickers hardness of martensite, defined by Eq. (1)
$\mathbf{K}$	stiffness matrix, see Eqs (5) and (6)
L_c	length of grinding zone, see Fig. 1
l_a	relative peak location of heat flux, $2\zeta_a/L_c$, see Fig. 1
M%	percentage of martensite phase
M_Y	yield stress of martensite, defined by Eq. (2)
P_e	Peclet number, $vL_c/4\alpha$
q	heat flux per unit grinding width
q_a	peak value of the heat flux, see Fig. 1
q_c	convection heat flux, hT_s, see Fig. 1
T	temperature rise with respect to ambient temperature T_∞(= 25°C)
T_s	instantaneous surface temperature rise of the workpiece
$\mathbf{u}$	displacement vector
v	moving speed of the heat source equal to the table speed of grinding, see Fig. 1
Y	yield stress of workpiece material
α	thermal diffusivity
σ	stress vector
$(\sigma_Y)_M$	instantaneous yield stress of the material undergoing phase transformation, defined by Eq. (3)
ϵ	strain vector
$\Delta()$	a small increment of quantity ()
κ	thermal conductivity of the workpiece material
Subscripts	
f	finish
m	mechanical
s	start
t	thermal
x,y,z	x-, y-, and z-directions, see Fig. 1
Y	yield
τ	time step
∞	room temperature
Superscripts	
i	step number of iteration
T	transpose

1. Introduction

The rapid heating and cooling in a grinding process may cause phase transformation and thermo-plastic deformation in a workpiece and in turn introduce substantial residual stresses. When phase transformation occurs, the properties of the workpiece material change. The extent of the change depends on the temperature history experienced, the instantaneous thermal stresses developed and the chemical compositions of the workpiece material. To carry out a reliable residual stress analysis, therefore, a comprehensive modelling technique and a sophisticated computational procedure, which can accommodate such property change in addition to the conventional thermo-plastic deformation, is required.

Although studies on residual stresses of phase transformation induced by grinding are lacking, there have been some relevant investigations in other areas. Using the finite element method, Murthy et al. [1] proposed an approach to investigate the residual stresses generated by welding and quenching. The nonlinearity due to variation of material properties, heat transfer coefficient, radiation boundary conditions and solid phase transformation were addressed. Ramakrishnan et al. [2] used the so-called inverse and direct methods to quantify the effects of phase change in quenching. Their inverse method utilized transient temperature measurements in the interior of a part to estimate the surface heat fluxes and heat transfer coefficients. Their direct method, however, used the estimated surface heat fluxes as boundary conditions for the heat transfer and thermal deformation analysis. These relevant studies indicate that numerical methods, such as the finite element method, can provide useful solutions to the residual stresses induced by phase transformation.

This paper aims to investigate the coupled effect of the conventional thermo-plasticity and the property change introduced by phase transformation associated with surface grinding processes. To this end, a feasible numerical method will also be developed with the aid of the finite element method.

2. Modelling

As shown in Fig. 1, the deformation of a workpiece subjected to a surface grinding operation is considered as a plane-strain problem. The heat generated by grinding is approximated by a triangular heat flux, q, moving along the positive direction of x-axis on the workpiece surface [3]. The apex strength of q is q_a. The base length of the flux is equal to the contact length, L_c, between the grinding wheel and workpiece. The apex location, ζ_a, is adjustable to account for the difference of flux distribution generated by down- and up-grinding operations. However, cooling through coolant with a convection flux q_c is considered to be proportional to the instantaneous surface temperature rise of the workpiece, T_s. In other words, the convection heat transfer coefficient of coolant is a constant over the whole workpiece surface.

2.1. Material properties

When a work material experiences a critical temperature change in grinding, phase transformation will take place [3,4]. Generally, martensite transformation will lead to the change of both

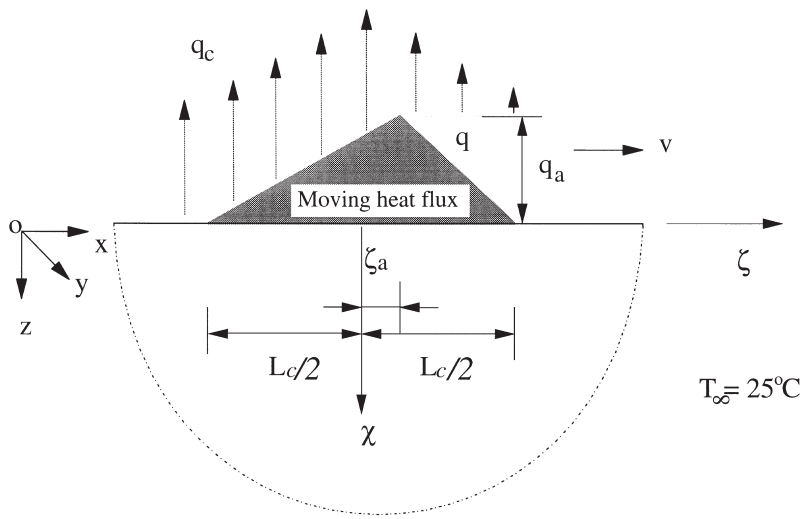

Fig. 1. Model of surface grinding.

mechanical and thermal properties of the material. To study the residual stresses of phase transformation by the finite element method, the first step is to have a suitable constitutive model that characterizes properly the behaviour of the workpiece material during phase transformation.

We propose the following constitutive model for the EN23 steel alloy [5] to describe the irreversible deformation induced by martensite transformation. The compositions and properties of the steel alloy are shown in Table 1. The variation of martensite hardness can be determined by the steel composition directly [6], i.e.

$$H_V = 463.24 + 21.00 \log(Cr_{700}), \tag{1}$$

where H_V is the Vickers hardness and Cr_{700} is the cooling rate at 700°C with the dimension of degree per hour. The yield stress of martensite, M_Y, can be calculated by

$$M_Y = 80.00 + 2.75H_V. \tag{2}$$

Table 1
The composition and mechanical properties of alloy steel EN23 [5]

Composition (% weight)						Yield stress (MPa)	Young's modulus (GPa)	Thermal coefficient of expansion (C^{-1})	Poisson's ratio
C	Si	Mn	Cr	Mo	Ni				
0.32	0.25	0.55	0.71	0.06	3.41	796	214	1.4×10^{-5}	0.27

The development of martensite depends on both the starting and finishing temperatures of transformation, M_s and M_f, as shown in Fig. 2. For the EN23 steel alloy, M_s = 300°C and M_f = 85°C, and martensite grows at a higher rate when temperature is high.

The yield stress of the work material undergoing phase transformation can then be described by a weighted average based on the percentage of martensite phase formed, M%, that is,

$$(\sigma_Y)_M = (M\%)M_Y + (1 - M\%)Y, \tag{3}$$

where $(\sigma_Y)_M$ is the instantaneous yield stress of the ground component undergoing phase change and Y is the yield stress of the material before phase transformation. Other properties of the material are considered unchanged in grinding.

2.2. Finite element analysis

2.2.1. Algorithm

To use the above constitutive model for residual stress analysis, we developed a special finite element code to determine the state of grinding temperature in relation to grinding conditions, to calculate the instantaneous mechanical properties at a given point in the workpiece and to perform the thermal stress analysis with a moving heat flux and coolant convection.

For an elastic-plastic deformation, the relationship between incremental strains and incremental stresses can be written as

$$\Delta\sigma = \mathbf{D}\Delta\epsilon \tag{4}$$

where $\mathbf{D}$ is the constitutive matrix [7], $\Delta\sigma$ is the incremental stress vector and $\Delta\epsilon$ is the incremental strain vector.

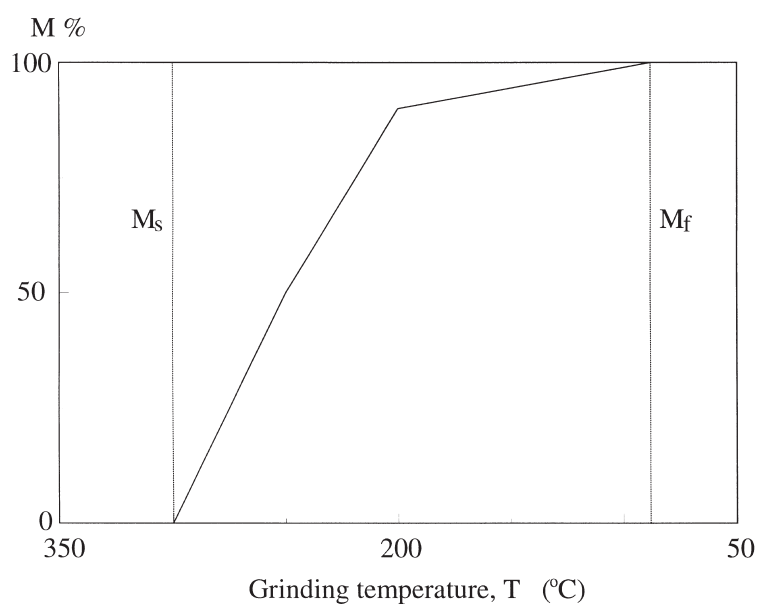

Fig. 2. Martensite formation curve of alloy EN23 [6].

At equilibrium the incremental nodal displacements, $\Delta\mathbf{u}$, and the incremental consistent nodal forces, $\Delta\mathbf{F}$, are related by the element stiffness matrix $\mathbf{K}$, i.e.

$$\mathbf{K}\Delta\mathbf{u} = \Delta\mathbf{F} \tag{5}$$

where

$$\mathbf{K} = \int \mathbf{B}^T \mathbf{D}\, \mathbf{B}\, \mathbf{dv} \tag{6}$$

$$\mathbf{F} = \int \mathbf{B}^T \mathbf{D}\, \epsilon_t\, \mathbf{dv} \tag{7}$$

in which $\mathbf{B}$ is the strain-displacement matrix and ϵ_t is the thermal strain vector defined by

$$(\epsilon_{ij})_t = \delta_{ij}\alpha T \tag{8}$$

where δ_{ij} is Kronecker delta, α is the coefficient of thermal expansion and T is the temperature rise with respect to ambient temperature T_∞.

To integrate the non-linear Eq. (5), a direct iterative procedure is implemented to meet the equilibrium conditions specified by a small relative error norm of displacement increments. Therefore Eq. (5) can be rewritten as

$$\mathbf{K}^{i-1}\Delta\mathbf{u}^i = \Delta\mathbf{F}^{i-1} \tag{9}$$

where i is the ith iteration number.

The updated displacement and stress vectors, $\mathbf{u}$ and σ, are therefore

$$\mathbf{u}_{\tau+1} = \mathbf{u}_\tau + \Delta\mathbf{u}_\tau \tag{10}$$

and

$$\sigma_{\tau+1} = \sigma_\tau + \Delta\sigma_\tau \tag{11}$$

where τ is the time step. Figure 3 shows the flowchart of the above algorithm.

2.2.2. Control volume and error analysis

A control volume of $16L_c \times 12L_c$ is selected for the analysis based on the criterion that boundary effect becomes negligible. In the finite element discretization, a finer mesh is used for the surface layer of 1 mm thick that may experience phase transformation. This layer is divided uniformly into eight sub-layers by 512 elements of four nodes. The total number of elements and nodes in the control volume are 832 and 910, respectively.

Theoretically, the cooling from a grinding temperature to room temperature is an asymptotic process and needs a huge number of time steps. To avoid this difficulty in numerical analysis, we assume, based on our numerical experiment considering both accuracy and computational cost, that after 70 time steps grinding temperature reduces linearly to room temperature (T_∞ = 25°C) in ten steps.

To confirm the reliability of the algorithm, the results of the present code are compared with those from ADINA [8] when grinding conditions are not critical[1]. Figure 4 shows that they are in close agreement.

[1] ADINA cannot directly deal with the change of material properties due to phase transformation. The comparison is therefore made under the conditions of no phase change.

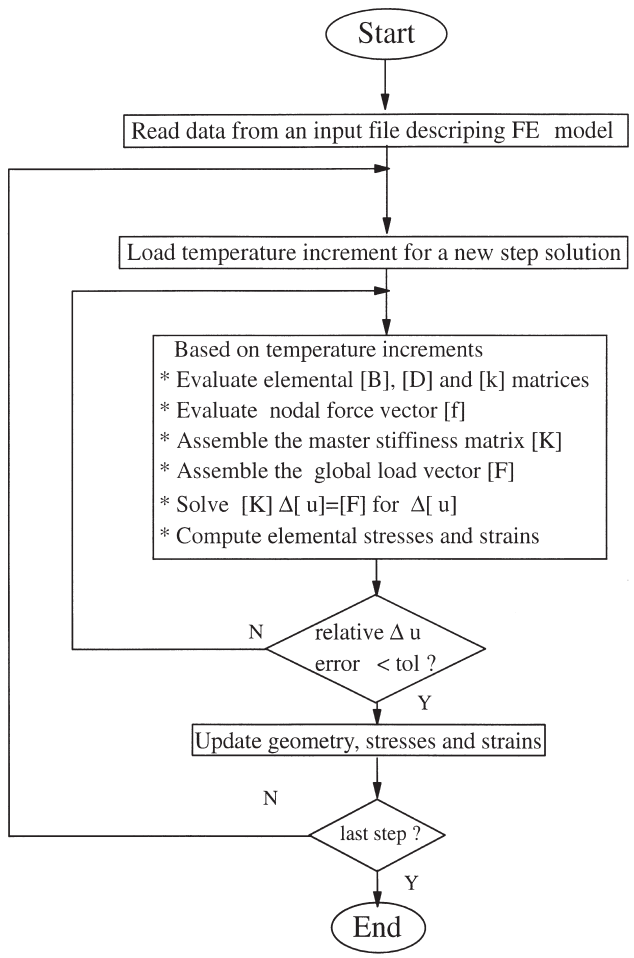

Fig. 3. Solution algorithm.

3. Results and discussion

The variations of surface temperature and yield stress of surface material with the motion of heat flux are demonstrated in Fig. 5, which shows the role of temperature history on the change of material properties caused by phase transformation. Surface temperature reaches its steady state in a short time (Fig. 5(a)). According to the surface temperature history and work material properties, martensite layer must appear. In the immediate layer underneath the ground surface ($z = 0$), the yield stress variation with martensitic phase is related to the motion of heat flux (Fig. 5(b)). The growth of martensite develops a hardened zone with a higher yield stress that expands with the movement of the heat flux. Because of this, the surface yield stress increases to $2.8Y$ (Fig. 5(b)). In the deeper subsurface of the work material, cooling rate is lower [4] and more time is required to initiate and complete the phase transformation. Therefore, in the transient stage of grinding, the thickness of martensite layer is non-uniform, as shown in Fig. 5(c).

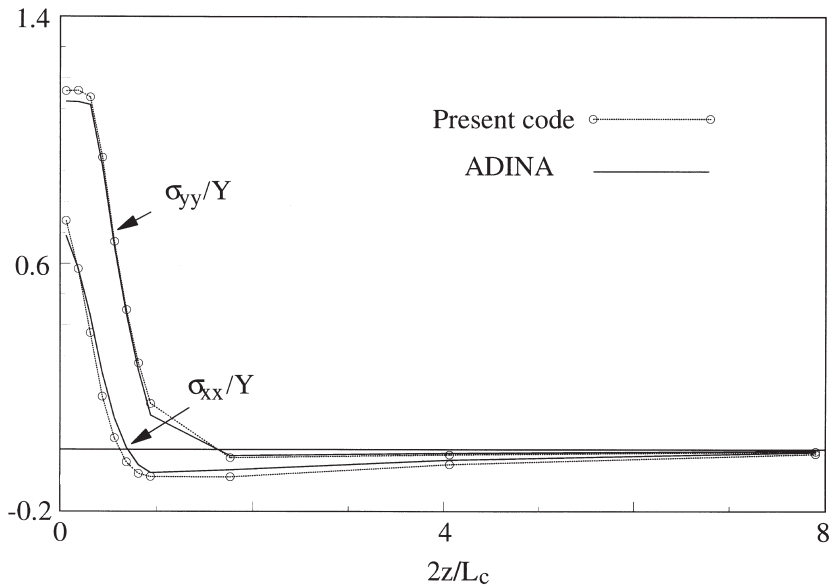

Fig. 4. Comparison of residual stress prediction for the cases without phase transformation (q_a = 80 MW/m^2, l_a = 0.25, Pe_∞ = 1, H_∞ = 0).

Figure 6 shows the effect of surface hardening on the variation of residual stresses when the volume of the work material is considered to be constant during phase transformation. In this case, both the residual stress components, σ_{xx} and σ_{yy}, are tensile with a maximum of 2.6 times the initial yield stress of workpiece material. Therefore surface hardening results in higher tensile surface stresses, since the yield stress of martensite is higher. The residual stresses near the surface vary almost linearly, but change rapidly near the interface between the martensite and no-martensite zones at the depth of D = 0.33. The effect of surface hardening on residual stresses becomes negligible in the region further away from the ground surface. This indicates that the variation of σ_{xx} and σ_{yy} inside the martensite zone is directly related to martensite depth. Therefore, an experimental measurement without sufficient attention to the depth of phase transformation may not provide a correct residual stress distribution.

When a volume growth of work material during phase transformation occurs, the nature of residual stresses could become very different. The permanent volume growth of martensite is restrained by the part without phase change and yields compressive residual stresses. Figure 7 illustrates the variation of σ_{xx} and σ_{yy} with volume growth when material properties are constant. The increase of martensite volume tends to generate more compressive surface residual stresses, but the jump from compressive to tensile at the martensite–nonmartensite interface also becomes sharper.

If martensite transformation takes place together with a volume increase, which is normally the case in practice, the variation of residual stresses is the resultant of the coupled effect of the above two. As shown in Fig. 8, under the coupled effect, surface hardening results in higher magnitudes of residual stresses regardless of their nature, i.e., compressive or tensile.

The role of up- and down-grinding processes can be examined qualitatively by varying the

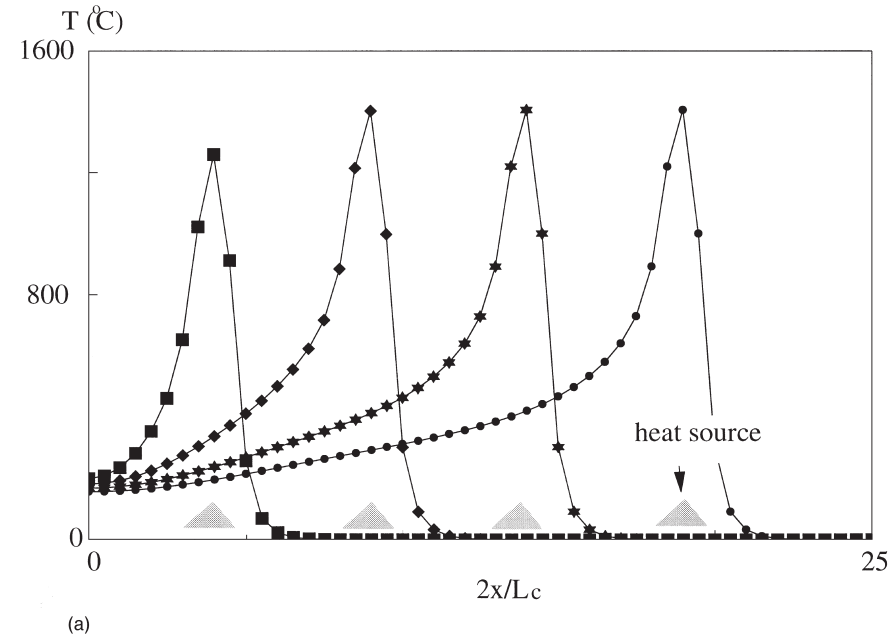

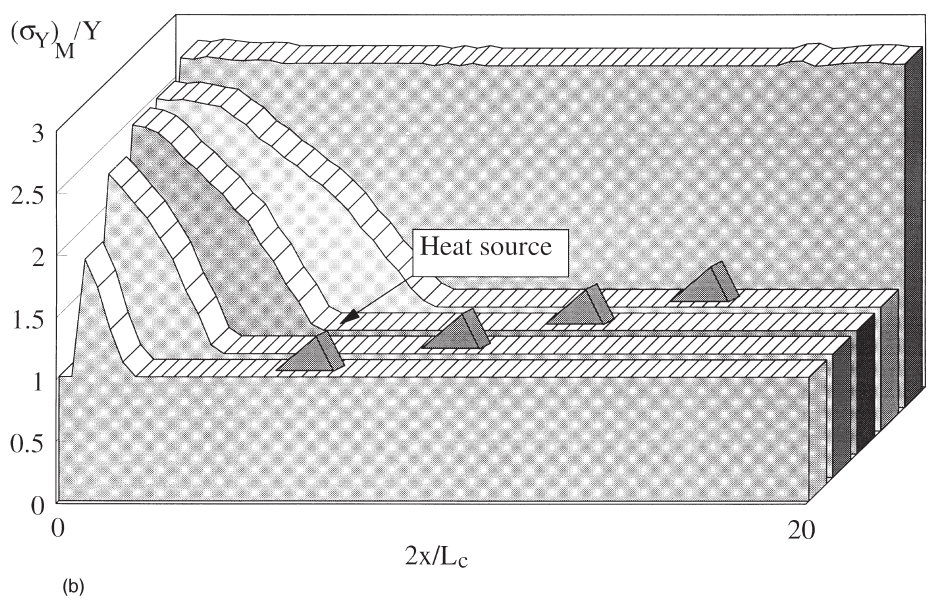

Fig. 5. Typical surface temperature and properties (q_a = 80 MW/m^2, l_a = 0.25, Pe_∞ = 1, H_∞ = 0). (a) Surface temperature, (b) surface hardening history at z = 0, (c) martensite development in the subsurface.

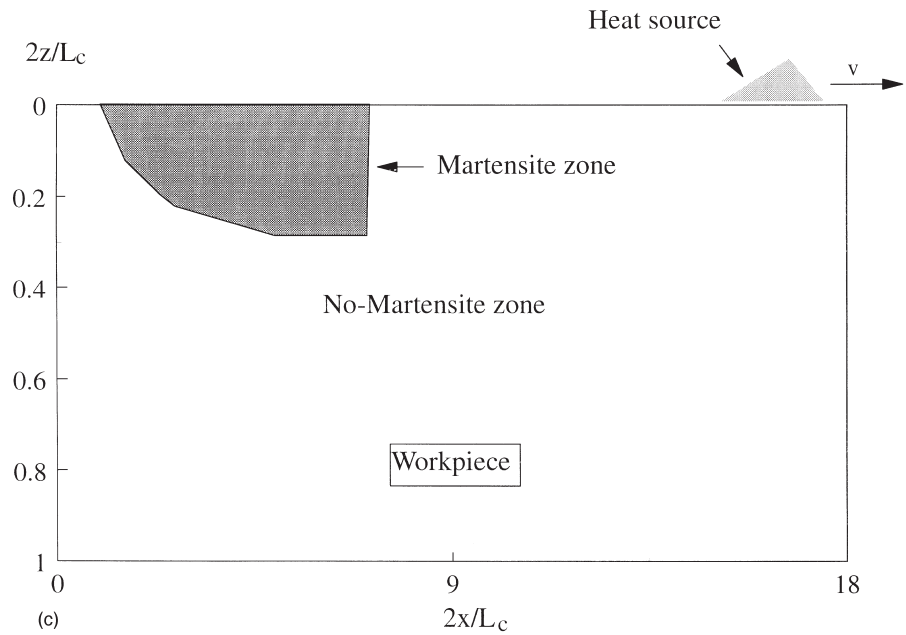

Fig. 5. Continued.

relative peak location of the heat flux profile, $l_a = 2\zeta_a/L_c$, see Fig. 1. As pointed out by Zhang et al. [9,10], an up-grinding normally gives rise to a smaller l_a ($0 < l_a < 0.5$), but a down-grinding yields a larger l_a ($0.5 < l_a < 1.0$). Figure 9 shows that $l_a = 0.25$ leads to a deeper penetration of tensile residual stresses. This is attributed to the higher temperature accumulated in the grinding zone and thereby generates a thicker martensite layer when all the other conditions are the same. Consequently, an up-grinding process results in a relatively greater depth of tensile residual stresses that is undesirable in practice. However, the surface residual stresses are not affected by up- or down-grinding processes.

Coolant plays a significant role in the formation of residual stresses, since surface cooling influences the grinding temperature history and thus alters the phase transformation process. Fig. 10 demonstrates that a higher cooling rate gives rise to a lower grinding temperature and thus a thinner martensite layer. If the grinding temperature is below the austenzing temperature, martensite will not form and residual stresses in this case will be caused only by the conventional thermoplastic deformation without phase change (i.e. with constant material properties). When a hardened martensite layer appears, residual stresses vary almost linearly in both the hardened and non-hardened zones. If the convection heat transfer coefficient, H, is low (e.g. $H = 0$ and 0.25 in this study), the maximum residual stress (MRS) is not affected much by cooling. When H is high, however, the effect of cooling on MRS becomes significant, since martensite depth is much thinner.

The strength of the grinding heat flux is another important factor that alters martensite formation in the grinding zone. Figure 11 shows that a weaker heat flux causes a lower grinding temperature, a thinner martensite layer and a smaller zone with residual tensile stresses. It confirms the previous observations that the penetration depth of residual tensile stresses is directly related to martensite

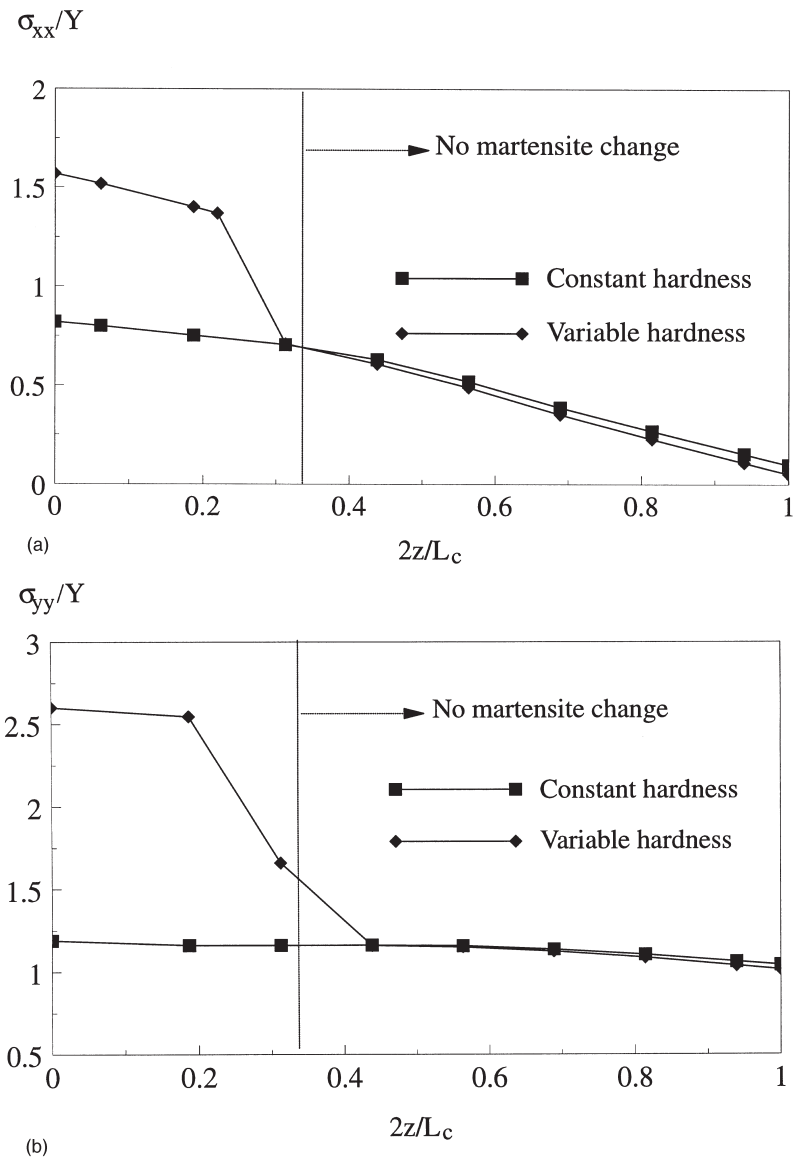

Fig. 6. Phase change and hardening effect on residual stresses (q_a = 80 MW/m^2, l_a = 0.25, Pe_∞ = 1, H_∞ = 0). (a) σ_{xx}, (b) σ_{yy}.

depth and the maximum residual stresses are not affected much by the strength of heat flux when it is beyond a critical level. In the present study, as shown in Fig. 11, the critical value of q_a in grinding the EN23 steel alloy is 60 MW/m^2.

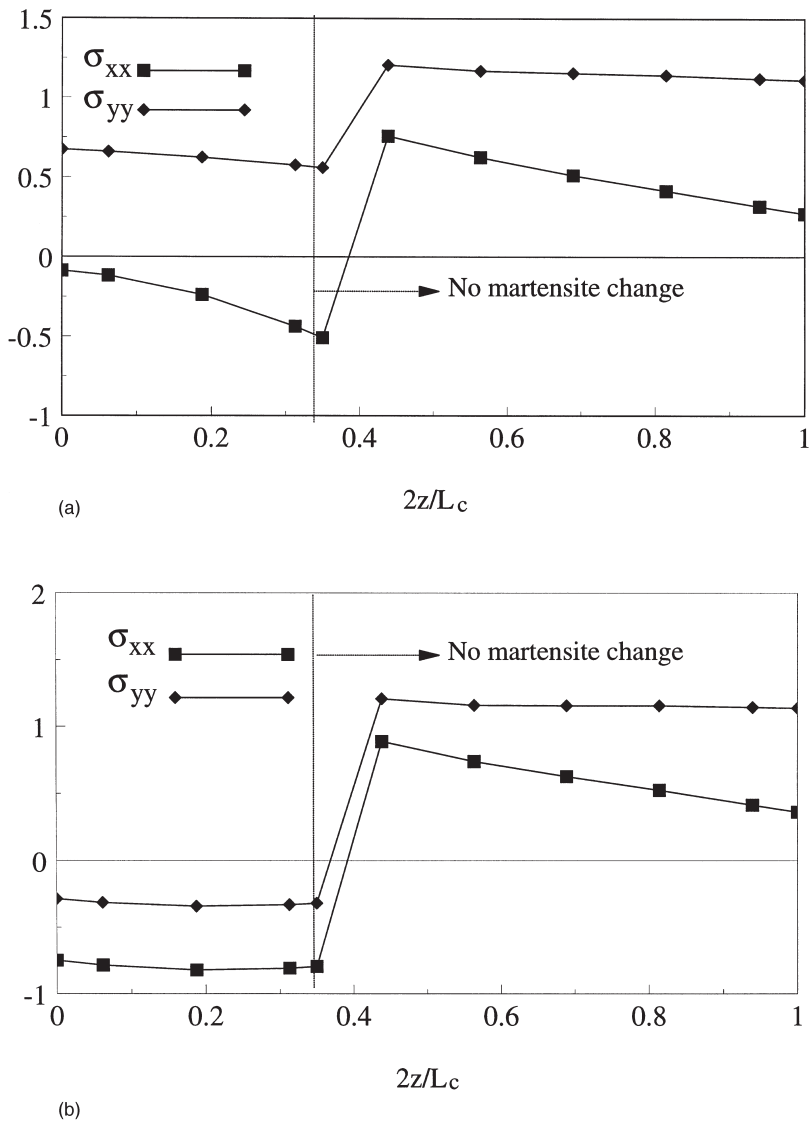

Fig. 7. Effect of volume growth on residual stresses (q_a = 80 MW/m^2, l_a = 0.25, Pe_∞ = 1, H_∞ = 0). (a) 2% volume growth, (b) 4% volume growth.

4. Conclusions

A simple material model and a stable numerical algorithm have been developed for studying the residual stresses and surface hardening induced by grinding when taking into account the coupled effect of phase transformation and thermo-plasticity. A systematic numerical investigation on grinding EN23 concludes that

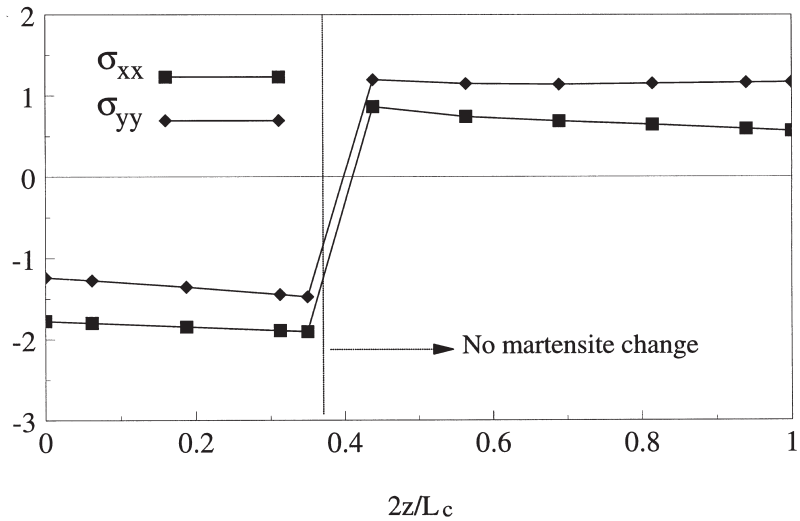

Fig. 8. Coupled effect of phase change and volume growth (q_a = 80 MW/m^2, l_a = 0.25, Pe_∞ = 1, H_∞ = 0, volume growth = 4%).

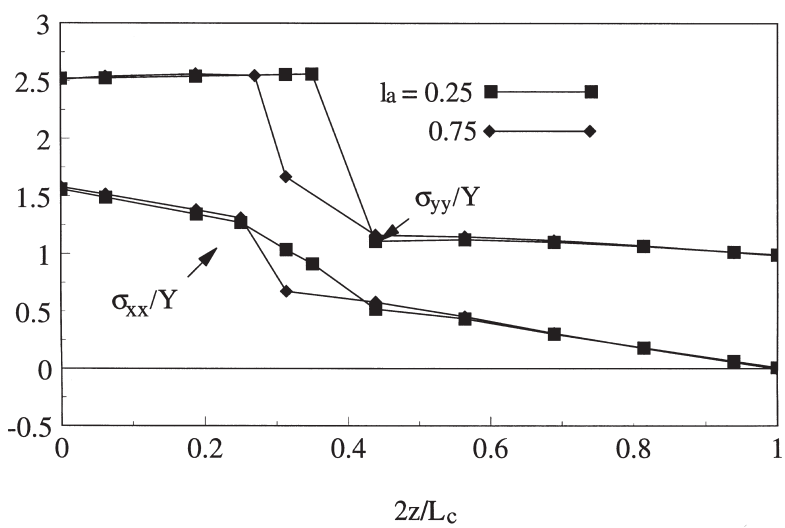

Fig. 9. Effect of up- and down-grinding on residual stresses (q_a = 80 MW/m^2, l_a = 0.25, Pe_∞ = 1, H_∞ = 0, volume growth = 4%).

1. surface hardening and volume growth due to phase transformation dominate the transition of residual stresses from compressive to tensile,
2. residual stresses in the no-martensite zone are nearly unaffected by surface hardening and volume change, and
3. the maximum surface residual stress is insensitive to cooling when the convection coefficient

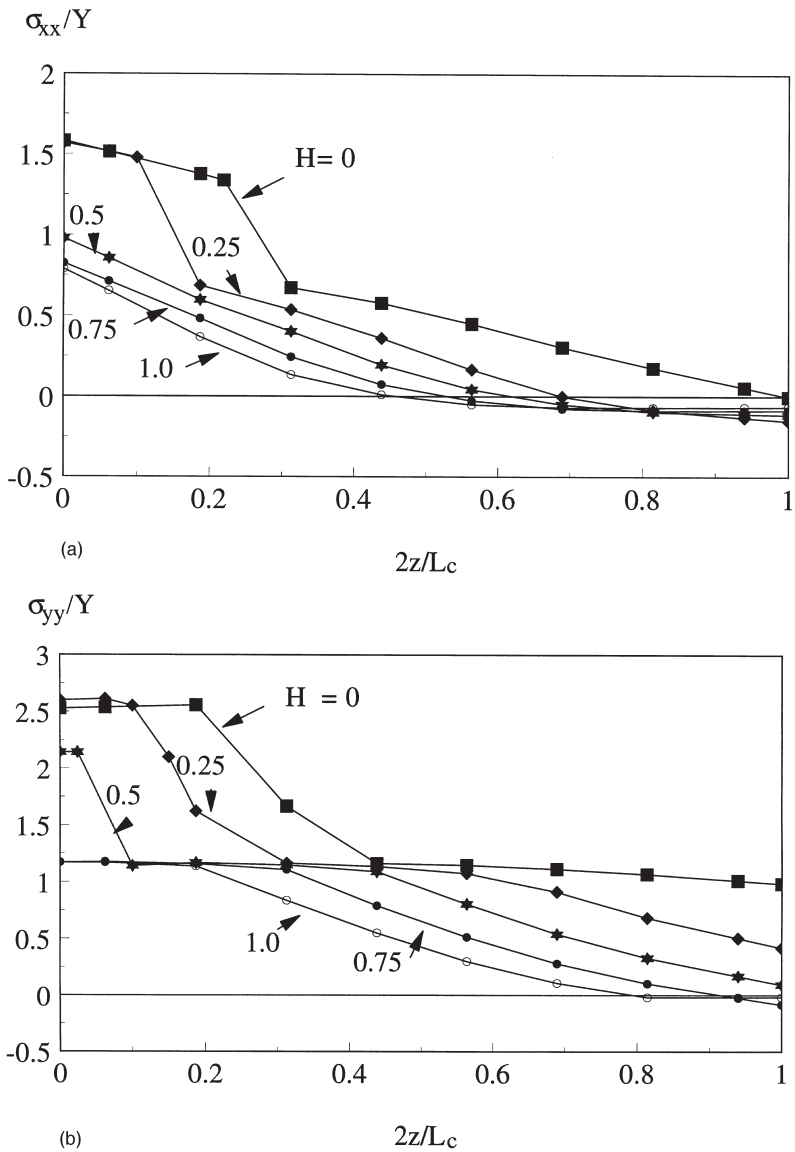

Fig. 10. Cooling effect on residual stresses (q_a = 80 MW/m^2, l_a = 0.25, Pe_∞ = 1, volume growth = 0%). (a) σ_{xx}, (b) σ_{yy}.

is below a certain value and is a weak function of the strength of heat flux when the strength is beyond a critical level.

Acknowledgements

The continuous support from Australian Research Council to the present study is greatly appreciated. ADINA code was used for grinding temperature calculations.

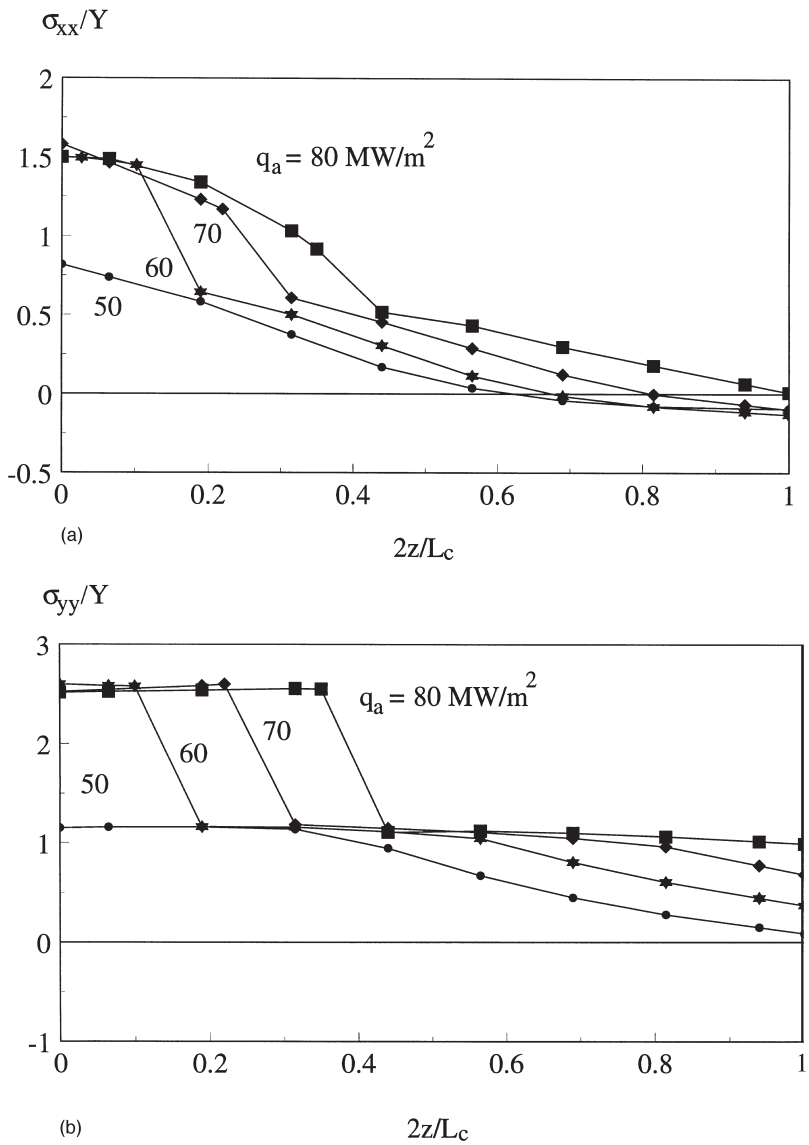

Fig. 11. Effect of strength of input heat flux (l_a = 0.25, Pe_∞ = 1, H_∞ = 0, volume growth = 0%). (a) σ_{xx}, (b) σ_{yy}.

References

[1] Y.V.L.N. Murthy, R.G. Venkata, P.K. Iyer, Numerical simulation of welding and quenching processes using transient thermal and thermo-elasto-plastic formulations, Computers and Structures 60 (1996) 131–154.
[2] R.I. Ramakrishnan, T.E. Howson, Modeling the heat treatment of superalloys, Journal of the Minerals, Metals and Materials Society 44 (June) (1992) 29–32.
[3] M. Mahdi, L.C. Zhang, The finite element thermal analysis of grinding processes by ADINA, Computers and Structures 56 (1995) 313–320.

[4] L.C. Zhang, M. Mahdi, Applied mechanics in grinding, part IV: grinding induced phase transformation, International Journal of Machine Tools Manufacture 35 (1995) 1397–1409.
[5] British Iron and Steel Research Association, The Mechanical and Physical Properties of the British Standard on Steels, Vol. 2, Pergamon Press, Oxford, 1969.
[6] M. Atkin, Atlas of Continuous Cooling Transformation Diagrams for Engineering Steels, British Steel Corporation, Sheffield, UK, 1977.
[7] K.-J. Bathe, Finite Element Procedures in Engineering Analysis, Prentice-Hall, New Jersey, 1982.
[8] ADINA R & D Inc., Theory and Modelling Guide, Report ARD 92-5, ADINA R & D Inc., December, 1992.
[9] L.C. Zhang, T. Suto, H. Noguchi, T. Waida, An overview of applied mechanics in grinding, Manufacturing Review 5 (1992) 261–273.
[10] L.C. Zhang, T. Suto, H. Noguchi, T. Waida, On some fundamental problems in grinding, in: M.H. Aliabadi, C.A. Brebbia (Eds.), Computer Methods and Experimental Measurements for Surface Treatment Effects, Computational Mechanics Publications, Southampton, 1993, pp. 275–284.